Interstitial cells from rat middle cerebral artery belong to smooth muscle cell type

Maksym I. Harhun [a], *, Kinga Szewczyk [b], Holger Laux [a], Sally A. Prestwich [a], Dmitri V. Gordienko [a, c], Ray F. Moss [b], Thomas B. Bolton [a]

[a] *Ion Channels and Cell Signalling Centre, Division of Basic Medical Sciences, St. George's, University of London, London, United Kingdom*
[b] *Image Resource Facility, Division of Basic Medical Sciences, St. George's, University of London, London, United Kingdom*
[c] *Department of Nerve-Muscle Physiology, Bogomoletz Institute of Physiology, Kiev, Ukraine*

Abstract

It is now established that non-contractile cells with thin filopodia, also called vascular interstitial cells (VICs), are constitutively present in the media of many, if not all, blood vessels. The aim of this study was to determine the type of cell lineage to which arterial VICs belong using immunocytochemical, and real-time and reverse transcription PCR (RT-PCR). Using RT-PCR, we compared gene expression profiles of single VICs and smooth muscle cells (SMCs) freshly dispersed from rat middle cerebral artery. Both VICs and SMCs expressed the SMC marker, smooth muscle myosin heavy chain (SM-MHC), but did not express fibroblast, pericyte, neuronal, mast cell, endothelial or stem cell markers. Freshly isolated VICs also did not express c-kit, which is the marker for interstitial cells of Cajal in the gastrointestinal tract. Immunocytochemical labelling of contractile proteins showed that VICs and SMCs expressed SM-MHC similarly to the same degree, but VICs in contrast to SMCs had decreased expression of α-SM-actin and very low or no expression of calponin. Real-time RT-PCR was consistent with immunocytochemical experiments and showed that VICs had four times lower gene expression of calponin comparing to SMCs, which may explain VICs' inability to contract. VICs had greater expression than SMCs of structural proteins such as non-muscular β-actin and desmin. The results obtained suggest that VICs represent a subtype of SMCs and may originate from the same precursor as SMCs, but later develop filopodia and a non-contractile cell phenotype.

Keywords: middle cerebral artery • smooth muscle cells • vascular interstitial cells • filopodia

Introduction

The wall of the blood vessel structurally consists of smooth muscle cells (SMCs), endothelial cells, neurons, fibroblasts, pericytes and connective tissue. Also cells, which are normally present in blood, such as monocytes, macrophages and lymphocytes, may be found in the adventitial layer of the vascular wall [1]. Although the media of the blood vessel is mainly populated by contractile SMCs, they, however, maintain considerable plasticity and can develop into a range of phenotypes especially in response to environmental stimuli [2]. Phenotypic modulation/switching of contractile SMCs into a different phenotype in response to environmental stimuli such as injury or disease is characterized by a dramatic increase in the rate of proliferation, migration and synthesis of extracellular matrix proteins and at the same time decreased expression of markers of mature SMCs such as smooth muscle α-actin (α-SM-actin), smooth muscle myosin heavy chain (SM-MHC), calponin, SM 22α and h-caldesmon [3]. It is noteworthy, however, that establishing the phenotype of SMCs is particularly challenging, because most SMC markers, which are selective in adult animals, are expressed, at least transiently, in other cell types during development, tissue repair or disease [3].

Recently, non-contractile cells with irregularly shaped body and long thin filopodia have been found in a number of vessels including veins [4] and arteries [5, 6] and are likely to be present in all blood vessels [6]. In contrast to mature contractile SMCs,

**Correspondence to: Dr. Maksym HARHUN,
Ion Channels and Cell Signalling Centre,
Division of Basic Medical Sciences, St. George's,
University of London, Cranmer Terrace, London, SW170RE,
United Kingdom.
Tel.: +44(0)20 87255653
Fax: +44(0)20 87253581
E-mail: m.harhun@sgul.ac.uk*

they varied in size, and normally represented about 5% of all cells in a suspension obtained by enzymatic digestion of a blood vessel. These cells were called VICs because of their morphological similarity to interstitial cells of Cajal (ICC), which play the role of pacemakers in the gastrointestinal tract [7]. Although the function of VICs is unknown, it is likely that in rabbit portal vein they can play a pacemaker role, because VICs, isolated from this vessel, generated rhythmical $[Ca^{2+}]_i$ oscillations associated with membrane depolarization [4, 8]. VICs were found to be located within the medial layer of blood vessels making contacts by means of filopodia with SMCs and other VICs [4, 6, 9]. Although immunocytochemical staining showed the expression of some SMCs markers in VICs [5, 10], in this work, in order to determine the lineage of VICs, we analyse the RNA obtained from single SMCs and VICs isolated from rat left and right middle cerebral arteries (RMCAs) for the presence of particular markers of different cell types, which might be present in the blood vessels. We also compared gene and protein expression for some structural and contractile proteins in both SMCs and VICs.

Methods

Cell preparation

Right and left middle cerebral arteries were removed from male Wistar rats (250–350 g, 35 animals, obtained from our animal facilities) immediately after they had been humanely killed by cervical dislocation followed by exsanguination, which was in accordance with the UK Animals (Scientific Procedures) Act 1986 (Schedule 1). The vessels were cleaned of adherent fat and single cells were obtained by enzymatic dispersion [4, 8] and allowed to settle down in experimental chambers in physiological salt solution (PSS, in mmol/l: KCl 6, NaCl 120, $MgCl_2$ 1.2, $CaCl_2$ 2.0, D-glucose 10, and HEPES 10; pH was adjusted to 7.3 with NaOH).

Scanning and transmission electron microscopy

For scanning electron microscopy (SEM), the isolated cells were fixed in 3% glutaraldehyde in cacodylate buffer, post-fixed in 1% osmium tetroxide, dehydrated through graded alcohols, critical point dried, mounted on aluminium stubs and sputter coated with gold. Samples were viewed with a Cambridge 360 scanning electron microscope (Cambridge Instruments, Cambridge, UK).

For transmission electron microscopy (TEM), the segments of the RMCAs were fixed in 3% glutaraldehyde in cacodylate buffer, post-fixed in 1% osmium tetroxide and dehydrated through graded alcohols. Then fragments were embedded in epoxy resin. Thin sections were cut at 90 nanometres using a diamond knife and mounted on uncoated 200 mesh copper grids. Differential staining of the tissue was achieved by floating the grids for 1 min. on a droplet of 10% potassium permanganate [11] in distilled water prior to post-staining with aqueous uranyl acetate and Sato's lead citrate and viewed with a Hitachi 7100 transmission electron microscope (Hitachi, Japan).

RT-PCR and real-time RT-PCR

For reverse trancription polymerase chain reaction (RT-PCR) and real-time RT-PCR, single SMCs and VICs (~150 cells each) were collected separately using a glass pipette attached to micromanipulator and frozen on dry ice immediately. For RT-PCR, total RNA was extracted using Qiagen RNeasy extraction kit (Qiagen, Crawley, UK). cDNA was obtained using Superscript II Reverse Transcriptase (Invitrogen, Paisley, UK) and used in PCR. cDNA was used as a template in 50 μl PCR reaction containing 1.5 mmol/l $MgCl_2$, 0.2 mmol/l deoxynucleoside triphosphates, 0.2 μmol/l forward and reverse primers (Invitrogen) and 2.5 units of platinum *Taq* DNA polymerase (Invitrogen). Amplification was performed according to the following schedule using a Touchgene Thermocycler (Techne, Cambridge, UK): 94°C for 2 min.; 35 cycles of 94°C for 30 sec.; 57°C for 60 sec.; and 72°C for 3 min., followed by a final elongation period of 10 min. at 72°C. No-template control PCR was also performed simultaneously with every reaction. Primers were designed so that they spanned at least one intron of the genomic sequence to avoid detecting genomic DNA contamination. The experiments were repeated with seven preparations of independently collected VICs and SMCs. The primers were designed to amplify the genes encoding proteins of interest. The PCR products were separated and visualized in ethidium bromide-stained 2% agarose gel by electrophoresis, extracted with gel extractions kit (Qiagen) and sequenced to confirm their identity. Considering that some products might not be detected after first amplification because of the small amount of initial cDNA, second PCR amplification was always performed, using products from first PCR amplification as a template. Second PCR amplifications confirmed the data from the first PCR and did not show the presence of additional products.

The following primers were used in these experiments (the data in the brackets will be as following: Genebank accession number, the sense bordering nucleotide position and the anti-sense bordering nucleotide position): β-actin (NM_031144, 306–325 and 862–881), smooth muscle myosin heavy chain for SMCs [12] (X16262, 447–466 and 1182–1191), c-kit for gastrointestinal ICC [13] (NM_022264, 862–881 and 1714–1733), protein gene product 9.5 for neurons [14] (D10699, 54–73 and 544–563), vascular endothelial growth factor A for endothelial cells [15] (NM_031836, 25–44 and 551–580), CD34 for endothelial cells and fibroblasts [16] (XM_223083, 218–237 and 1050–1069), prolyl-4-hydroxylase for fibroblasts [17] (NM_012998, 571–570 and 1359–1378), CD68 for macrophages [18] (BC098931, 143–162 and 925–944), NG2 proteoglycan for pericytes [19] (NM_031022, 1815–1834 and 1991–2810), prominin 1 for stem cells [20] (NM_021751, 312–331 and 1183–1192), mast cell carboxypeptidase A for mast cells [21] (U67914, 118–137 and 996–1115), α-SM-actin (NM_031004, 164–183 and 697–714), calponin (NM_031747, 162–181 and 776–795).

Comparison of calponin transcript abundance relative to β-actin message in both separately collected SMCs and VICs was performed using real-time RT-PCR. For this, corresponding RNA was reversely transcribed with oligo (dT) primers using the AffinityScript qPCR cDNA synthesis kit (Stratagene, Cedar Creek, TX, USA). As our cDNA samples were very limited (the corresponding RNA was isolated out of ~150 cells), we performed preamplification of the cDNA using the TaqMan® PreAmp Master Mix kit (Applied Biosystems, Foster City, CA, USA) following the manufacturer's guidelines. Fourteen amplification cycles were performed and the preamplification product was diluted 1:20 in TE buffer afterwards. Real-time RT-PCR was carried out in the Mx3000 (Stratagene) using the Taqman Universal PCR Mastermix (Applied Biosystems). Assay-on-demand (predesigned primer and probe sets for Calponin and β-actin (3 prime located; spanning exon-intron boundary) was applied for quantitative real-time PCR reactions according to the procedure described by the manufacturer

(Applied Biosystems). β-actin was used as a calibrator. Thermal cycling was one step at 50°C for 2 min., 95°C for 10 min., followed by 40 cycles at 95°C for 15 sec. and 60°C for 1 min. Results were analysed with Stratagene Mx3000P software. Two technical and two biological replicates were used. The relative amount of target mRNA was determined using the comparative threshold (Ct) method by normalizing target mRNA Ct values to those for β-actin (delta Ct).

Immunocytochemistry

Single cells or segments of RMCAs were fixed with 4% formaldehyde solution at 4°C for 4 and 15 min., respectively, washed with PSS and incubated with PSS containing 2% bovine serum albumin (BSA) and 0.3% Triton X-100. Then samples were incubated with primary antibodies in PSS containing 2% BSA overnight at 4°C, washed with PSS and incubated for 2 hrs with secondary antibodies conjugated with fluorescent probes. Samples were washed with PSS, and viewed using the laser scanning confocal microscope Zeiss LSM 510 (Carl-Zeiss GmbH, Jena, Germany).

In our experiments, the following antibodies were used: β-actin: mouse monoclonal (clone AC-15, dilution 1:400); desmin: mouse monoclonal (clone DE-U-10, dilution 1:300) all from Sigma-Aldrich (Dorset, UK); vin-culin: mouse monoclonal (hVIN-1, dilution 1:300); α-actinin: rabbit poly-clonal (dilution 1:300), SM-MHC: mouse monoclonal (1G12, dilution 1:300); α-SM-actin (1A4, dilution 1:400, SIGMA), calponin: mouse mono-clonal (CALP, dilution 1:300) all from Abcam (Cambridge, UK); PE-Cy7Conjugated Anti-mouse c-kit (2B8, dilution 1:300, eBioscience, San Diego, CA, USA); Alexa Fluor 488 chicken anti-mouse IgG (dilution 1:400, Invitrogen); MFP488 goat anti-mouse IgG (dilution 1:400); MFP555 donkey anti-rabbit IgG (dilution 1:400) both from Mobitec (Göttingen, Germany).

Confocal imaging data were processed and analysed using Zeiss LSM software. An image taken approximately in the middle of the cell was selected out of the z-stack of horizontally taken images [10]. Using such an image the average pixel fluorescence (APF) was calculated according to equation:

$$AFP = \frac{\sum i(p)}{n(p)} \text{ (intensity units/pixel)}$$

where $i(p)$ is the intensity of a pixel within the confocal plane of the cell, and $n(p)$ is the total number of pixels of the plane. Statistical evaluation and graphs were created using MicroCal Origin, (Origin Lab Corporation, Northampton, UK) and final images were produced using Corel Draw7, (Corel Corporation, Ottawa, Canada).

Statistical analysis

All data are shown as a mean ± S.E.M. for the number of cells (n) analysed. Statistical significance was calculated using Student's t-test for paired observations and the differences where $P < 0.05$ were considered significant.

Results

Following upon enzymatic digestion of RMCAs, we observed het-erogeneity of cells in suspension. Apart from isolated SMCs and
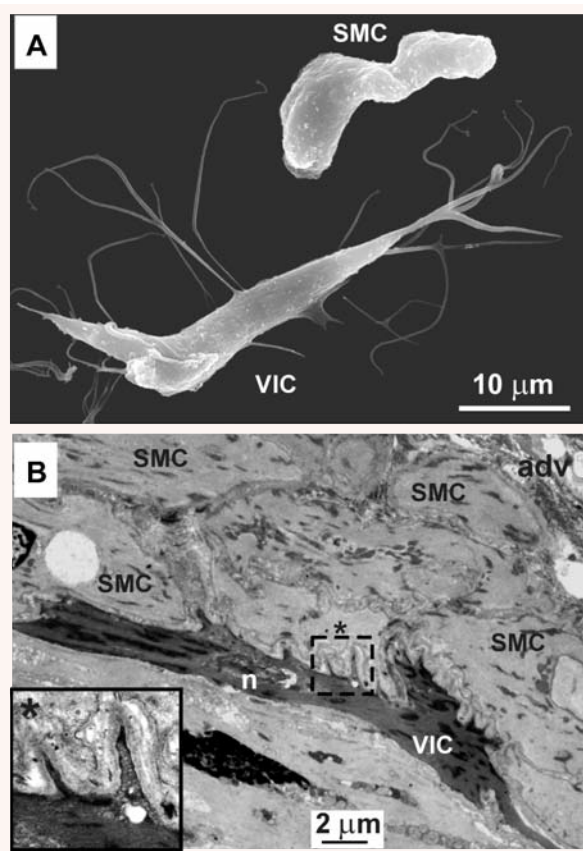

Fig. 1 Vascular interstitial cells of the RMCAs revealed by electron microscopy. (**A**) Scanning electron micrograph of enzymatically isolated VIC and SMC. (**B**) Transmission electron micrograph of the cross-cut section of the RMCAs displaying a VIC (the darker cell with thin multiple filopodia). The dashed rectangular region of the image with some of the filopodia of the VIC is shown enlarged. Adv – adventitia of the vessel and n – nuclei of the VIC.

occasional red blood cells, we also observed cells with irregular body shape and multiple long thin filopodia. These cells were quite abundant and constituted up to 5% of the total cells in the dispersal. In contrast to single SMCs, these cells did not contract in response to application of caffeine (5 mmol/l) or rupture of the plasma membrane with a glass micropipette. Cells with similar properties were observed in our previous research [6, 22] and were called VICs by analogy with the gut ICCs because of their morphological similarities. An example of an SEM micrograph of single isolated VIC and SMC is shown in Fig. 1A. Initially, it was difficult to identify these cells in TEM cross-sections of the vessel. However, additional treatment with potassium permanganate to enhance contrast of the samples [11] revealed VICs in the media of this blood vessel as irregularly shaped darker cells with filopo-dia (Fig. 1B).
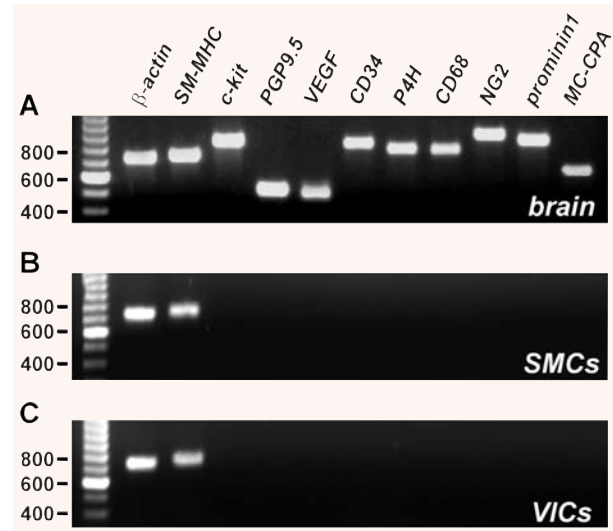
A TEM study showed that VICs have nuclei often with more than one lobe, some cisternae of smooth and rough endoplasmic
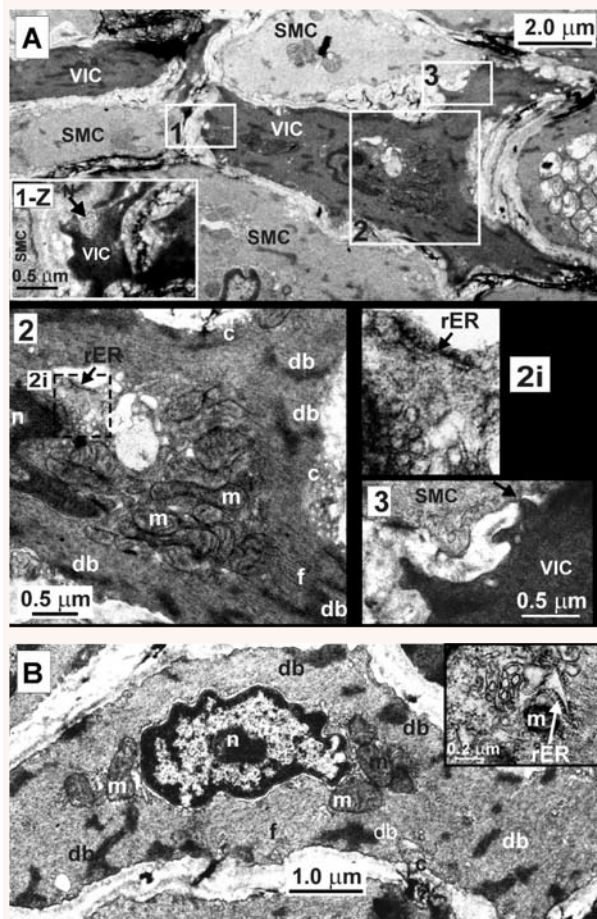
Fig. 2 The morphological characteristics of VIC (**A**) and SMC (**B**) from RMCAs revealed by TEM. Approximate cross-section of rat middle cerebral artery. **A1-Z** depicts the same area as **A1** but the section has been moved 2 microns along the z-axis. It demonstrates that a VIC is in close contact with a nerve fibre (N). **A2** shows the nucleated portion of a VIC containing the nucleus (n) and multiple mitochondria (m), caveolae (c), cisternae of smooth and rough endoplasmic reticulum (rER) (the latter shown enlarged in A2i), dense bodies (db) and filaments (f). **A3** shows that VIC forms a cell-to-cell contact with SMC (indicated by arrow). **B** shows a section of a SMC. Inset (top, right) shows the nucleated portion of a different SMC where the Golgi apparatus and rER cisternae are located.


Fig. 3 RT-PCR from separately collected VICs and SMCs shows that VICs from RMCAs express SMC marker. The following primers were designed to amplify genes associated with certain cell types: SM-MHC (745 bp) for SMCs, c-kit (861 bp) for ICCs, PGP9.5 (510 bp) for neurons, VEGF A (556 bp) for endothelial cells, CD34 (852 bp) for fibroblasts and endothelial cells, P4H (808 bp) for fibroblasts, CD68 (802 bp) for macrophages, NG2 (996 bp) for pericytes, prominin 1 (881 bp) for stem cells, MC-CPA (998 bp) for mast cells. As a positive control primers for β-actin (721 bp) were used. (**A**) Primers were tested for their specificity using cDNA preparations of rat brain tissue. (**B**) SMCs showed the presence of the β-actin and SM-MHC. (**C**) Isolated VICs also showed the expression of SMC marker only suggesting that they belong to SMC type.

reticulum (rER), and multiple mitochondria mainly located in the nucleated region of the cell (Fig. 2A). Numerous dense bodies and filaments were also observed. It was found that VICs have numerous caveolae all along the plasmalemma. Moreover, VICs were located in close proximity to nerve fibres (Fig. 2A, inset 1-Z) and formed cell-to-cell junctions with nearby SMCs (Fig. 2A, inset 3). SMCs also had nuclei often having more than one lobe and on average fewer mitochondria than VICs (Fig. 2B), as well as cisternae of sER and rER (Fig. 2B, inset). SMCs also had filaments directed along the longitudinal axis of the cell and dense bodies, most of which were located close to the periphery of the cell. SMCs had fewer caveolae than VICs.

It was possible to collect VICs and SMCs separately with a wide tip (10–20 μm) glass pipette, which allowed analysis for the presence of mRNA for markers for various cell types using RT-PCR technique. We designed a number of primers for genes encoding proteins considered to be specific for a particular cell type: for SMCs we used SM-MHC, for gastrointestinal ICC- c-kit, for neurons-PGP9.5, for endothelial cells – vascular endothelial growth factor A (VEGFA), for fibroblasts/endothelial cells – CD34, for fibroblasts – prolyl-4-hydroxylase (P4H), for macrophages – CD68, for pericytes – NG2, for stem cells – prominin 1, for mast cells – carboxypeptidase A (MC-CPA). Firstly, the specificity of the primers was confirmed by using a cDNA preparation from rat brain tissue (Fig. 3A). The cDNA preparation obtained from single SMCs isolated from RMCAs showed the presence of mRNA encoding only SM-MHC, which we used as a SMC marker (Fig. 3B). Subsequently, identical experiments involving single VICs showed the presence of SM-MHC only, similarly to SMCs (Fig. 3C).
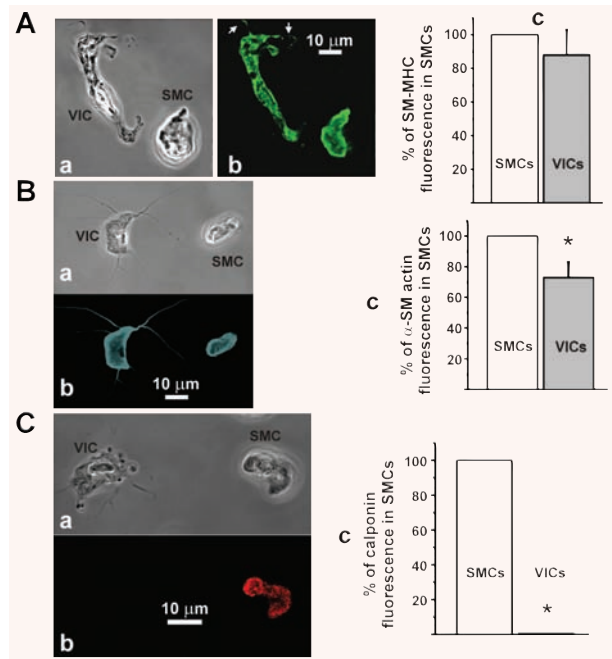
We found VICs to express the SMCs marker SM-MHC, but since they appear morphologically different from contractile SMCs, we studied the organization of some structural proteins in
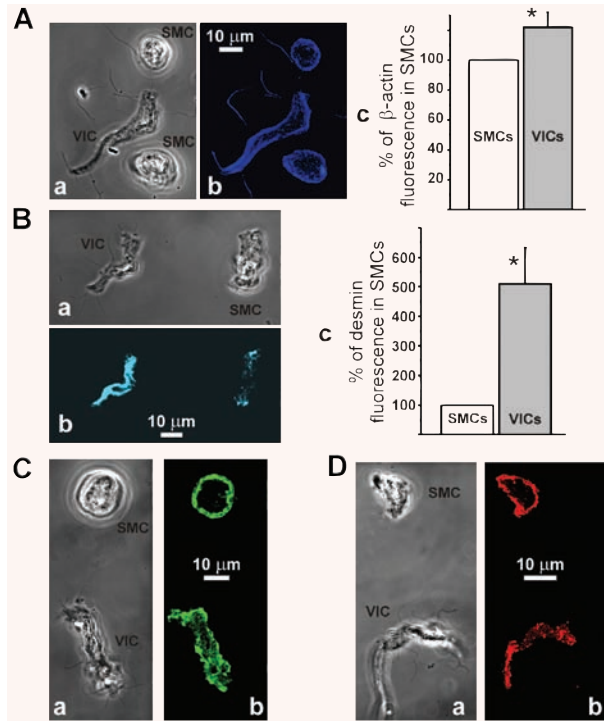
Fig. 4 Immunocytochemical staining of structural proteins in both SMCs and VICs from RMCAs. (**A**) VICs and SMCs when stained for β-actin and shown in transmitted light (**a**) and in fluorescent images (**b**) show a significant difference in fluorescence (**c**) with 121 ± 10% ($n = 7$ pairs, $P < 0.05$) of average pixel fluorescence in VICs to that in SMC. (**B**) When stained for desmin (transmitted light and fluorescent images are shown in (**a**) and (**b**), respectively) VICs displayed much higher fluorescence with 510 ± 122% ($n = 8$, $P < 0.0001$) in VICs to that of SMCs (**c**). Staining for 'anchorage' proteins vinculin (**C**) and α-actinin (**D**) (transmitted light images of cells shown in **Ca** and **Da**, respectively) showed similar regional difference between VICs and SMCs in the distribution of both these proteins (fluorescent images shown in **Cb** and **Db**). In VICs fluorescence indicated that these proteins are distributed nearly homogenous throughout intracellular space (with slightly lower fluorescence in the perinuclear region of the cells), however, in SMCs they were expressed mostly in the peripheral region of the cell.

Fig. 5 Immunocytochemical staining of contractile proteins in both SMCs and VICs from RMCAs. (**A**) VICs and SMCs stained for SM-MHC (transmitted light and fluorescent images are shown in (**a**) and (**b**), respectively) showed no significant difference in fluorescence with 88 ± 20% ($n = 7$, $P > 0.05$) in VICs of that in SMCs (**c**). Arrows in **Ab** point to filopodia of VIC. (**B**) VICs and SMCs stained for α-SM-actin (transmitted light and fluorescent images are shown in (**a**) and (**b**)) showed significantly less fluorescence in VICs with 73 ± 10% ($n = 8$, $P < 0.05$) of that in SMCs (**c**). (**C**) Staining of single cells for calponin (transmitted light and fluorescent images are shown in (**a**) and (**b**)) showed that VICs express a very low amount of this protein with average pixel fluorescence of 0.004 ± 0.002% ($n = 9$, $P < 0.05$) of that of SMCs (**c**).

of the laser of the confocal microscope within the range of our usual experimental parameters.

We also analysed expression of α-actinin and vinculin in both SMCs and VICs; these proteins are considered to be important in the anchorage of actin filaments to the plasma membrane [25]. Both of these proteins showed similar distribution in SMCs where they were located mainly on the periphery of the cells (Fig. 4C and D). In contrast, in VICs these proteins were distributed almost homogenously throughout the intracellular space with slightly lower concentration in the nuclear region of the cells (Fig. 4C and D).

Because VICs from RMCAs were found to be non-contractile, we analysed the expression of proteins participating in the contraction of SMCs. SM-MHC is considered as the most selective marker for SMCs; its presence has not been recorded in non-SMC types of cells [26]. Labelling of the suspension of the cells with anti SM-MHC antibody showed no significant difference in fluorescence for SM-MHC with 88 ± 20% ($n = 7$, $P > 0.05$) in VICs of that in SMCs suggesting a similar level of expression of this protein in both cell types (Fig. 5A). The fluorescence of the SM-MHC was also detected in filopodia of VICs (Fig. 5Ab).

SMCs *versus* VICs. Both types of cells stained positively for non-muscle β-actin with higher fluorescence in VICs 121 ± 10% ($n = 7$ pairs, $P < 0.05$) compared to that of SMCs (Fig. 4A). This protein was distributed throughout the whole cell in both SMCs and VICs, including filopodia of VICs, with a higher concentration at the periphery of the cells (Fig. 4Ab).

The intermediate filament protein desmin is considered to be present exclusively in muscle and endothelial cells [23]. Desmin is also absent in fibroblasts and myofibroblasts [24], which can be morphologically similar to our VICs. Labelling a single cell suspension for desmin revealed significantly higher fluorescence in VICs, with an average of 510 ± 122% ($n = 8$, $P < 0.05$) compared to that of SMCs (Fig. 4B). The expression of the desmin in the filopodia of VICs is likely to be very low, so the desmin fluorescence in thin filopodia could not be detected using the power

Fig. 6 Analysis of gene expression of contractile proteins in isolated SMCs and VICs from RMCAs. (**A**) Primers for α-SM-actin (product size 550 bp) and calponin (product size 633 bp) were tested on rat brain tissue by RT-PCR (**a**); RT-PCR showed that both SMCs (**b**) and VICs (**c**) express α-SM-actin and calponin. As a positive control primers for β-actin (721 bp) were also used. (**B**) (**a**) Real-time RT-PCR amplification graph shows a plot of number of cycles *versus* fluorescence for the genes calponin and β-actin for VICs and SMCs. The fluorescence data are baseline-corrected, normalized and averaged. Whereas there was no significant difference in β-actin expression between VICs and SMCs, there was a clear difference between VICs and SMCs for calponin. (**b**) VICs expression of calponin was $27 \pm 5\%$ ($n = 4$, $P < 0.05$) to that of SMCs.
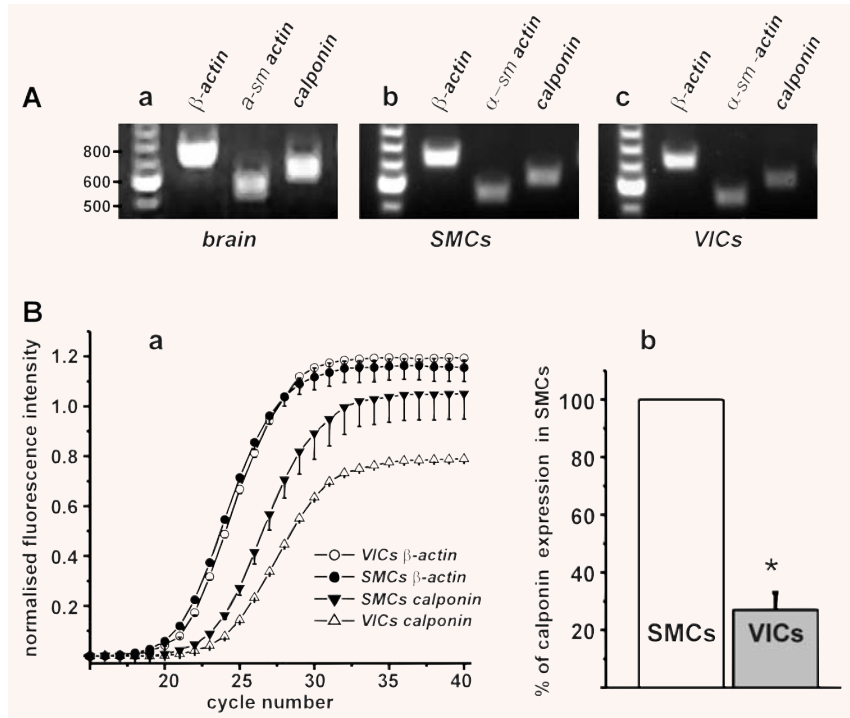
α-SM-actin is another protein of the contractile apparatus of SMCs [27] and commonly used as a marker of SMC differentiation [3]. The expression of α-SM-actin was found to be higher in SMCs with mean pixel fluorescence in VICs of $73 \pm 10\%$ ($n = 8$, $P < 0.05$) of that in SMCs (Fig. 5B). The fluorescent signal was stronger in the periphery of VICs and was also observed in filopodia of VICs (Fig. 5Bb).

A major actin-binding protein of smooth muscle, calponin, occurs both in the cytoskeleton and contractile apparatus of SMCs [27]. Immunostaining of the cell suspension obtained from RMCAs with anti-calponin antibodies showed almost undetectable fluorescence in VICs for calponin with mean pixel fluorescence of $0.004 \pm 0.002\%$ ($n = 9$, $P < 0.05$) of that of SMCs suggesting very low or no expression of this protein in VICs (Fig. 5C).

Using RT-PCR from single cells we confirmed the presence of the mRNA encoding α-SM-actin and surprisingly, calponin in both SMCs and VICs (Fig. 6A). Since RT-PCR does not truly reflect quantitative differences in gene expression and our immunostaining data suggested very low expression of the protein calponin in VICs comparing to SMCs (Fig. 5C), we compared gene expression for calponin in SMCs and VICs using real-time RT-PCR. The latter showed that the expression of calponin was almost four times lower in VICs than in SMCs (Fig. 6B).

Discussion

During the last few years, there have been only a few reports of the presence of VICs in a few blood vessels, including veins [5, 9] and

arteries [5, 6, 28]. Cells with the filopodia, also called as interstitial Cajal-like cells, were found in rat mesentery in close proximity to blood capillaries [29]. TEM of cross-sections of segments of rabbit portal vein [6], guinea pig mesenteric [10] and RMCAs confirmed that cells displaying long filopodia are found within the blood vessel wall. Hence filopodia are not developed after cell isolation. When a blood vessel is dispersed with proteolytic enzymes, VICs normally represent on average about 5% of all cells in the dispersal, although considering that VICs are more liable to be damaged during the mechanical part of the cell isolation procedure because of the presence of long thin filopodia, this number may be substantially higher.

We observed irregularly shaped cells with filopodia within the intact smooth muscle layer of the RMCAs with similar morphology to the cells with filopodia, which were found in the dispersal of the cerebral artery. The TEM showed that VICs were located in close proximity to nerve fibres and were making cell-to-cell contacts with SMCs. This, however, requires further study.

A few types of cell found in blood vessels with filopodia/processes are mainly associated with a different part of the blood vessel wall. Thus neurons, macrophages, fibroblasts and pericytes (found only in arterioles and capillaries) are normally associated with the adventitia of the vessel wall [1, 19]; however partially contractile myofibroblasts can be found in the media because of their migration from the adventitial layer of the blood vessel [1, 24]. To identify the lineage of VICs from RMCAs we performed RT-PCR using a number of cell-specific primers, trying to cover the whole spectrum of such cells.

Table 1 Comparison of the expression of proteins based on immunofluorescence data in isolated VICs and synthetic SMCs from the literature

	VICs% (SMCs = 100%)	Synthetic SMC
SM-MHC	88 ± 20%	Decreased expression [2]
α-SM-actin	73 ± 10%*	Decreased expression [2]
MLCK	32 ± 7% [10]*	Decreased expression [2]
Calponin	0.004 ± 0.002%*	Decreased expression [2]
β-actin	121 ± 10%*	Increased expression [2]
desmin	510 ± 122%*	Decreased expression [30]
smoothelin	21 ± 9% [10]*	Decreased expression [2]

MLCK and smoothelin data were used from our previous publication [10]. VICs express more desmin and the same amount of SM-MHC compared to the contractile SMC phenotype. They differ from synthetic SMCs by increased expression of desmin. *indicates the data with significant difference in immunofluorescemce between VICs and SMCs ($P < 0.05$).

Our results obtained using RT-PCR from separately collected SMCs and VICs showed that VICs, similarly to SMCs, express SM-MHC, which to date is considered as the best marker for SMCs [3]. VICs expressed neither markers for neurons nor for fibroblasts, the types of cells with closest morphological similarities to VICs. These cells also did not express the haematopoietic stem cell marker CD34, which is expressed by both fibroblasts and endothelial cells suggesting that VICs and SMCs likely originate from the same precursor. The absence in VICs of *c-kit*, which is the marker for ICC [13], suggested that this marker cannot be used universally for identification of cells resembling interstitial or Cajal-like cells as found in rabbit portal vein [4, 9]. In addition, labelling of fragments of RMCAs with anti-c-kit antibody showed no evidence of c-kit positive cells in the media of this vessel (data not shown).

VICs from RMCAs were found to be non-contractile cells. However, they express some proteins participating in SMCs contraction such as SM-MHC and α-SM-actin. Calponin is considered as a regulatory protein for SMC contraction [27], and our immunostaining showed that there was very little or no expression of this protein in VICs, which may in part explain the non-contractility of these cells, although low levels of mRNA for calponin were detected in VICs. Immunostaining of VICs and SMCs dispersed from guinea pig mesenteric artery also detected only a small amount of myosin light chain kinase (MLCK), the critical enzyme in the regulation of the smooth muscle contraction, in VICs comparing to SMCs [10].

The transformation of contractile SMCs to 'synthetic' phenotype in response to external factors [2] or in the culture [30] is characterized by a decrease in the expression of smooth muscle-specific proteins and an increase in non-muscle structural proteins. Non-contractile VICs show some similarities with 'synthetic' (non-contractile) type of SMCs (please see Table 1 for generalized

comparison). They have an increased level of β-actin, and decreased level of α-SM-actin and calponin. Interestingly, the expression of desmin during phenotypic modulation of SMCs is decreased [30], whereas VICs from RMCAs had a 5-fold higher fluorescence for desmin immunolabelling (Table 1). This may suggest that VICs represent another subtype of SMCs, different from the known 'synthetic' SMC subtype. In addition, the cells with long (tens of microns) thin filopodia have not been described in phenotypically differentiated SMCs either in healthy [31] or in atherosclerotic [32] vessels or in cultured [30, 33] SMCs, which also adds to the idea of the unique identity of VICs in blood vessels.

The presence of a substantial population of VICs within the media of blood vessels raises the question of their function. In the rabbit portal vein VICs were shown to participate in the generation of the pacemaker activity of this vessel [4, 8]. The role of VICs is obscure in cerebral arteries, because they are not constantly rhythmically active blood vessels. However, spontaneous vasomotion occurs quite often in the cerebral circulation [34–36]. It was found in our preliminary research that some VICs isolated from guinea pig middle cerebral artery and loaded with calcium indicator fluo 3 generated rhythmical calcium oscillations ($n = 3$, M Harhun, unpublished observations), similar to those observed in rabbit portal vein [8], which may suggest that VICs can participate in the generation of rhythmical activity in arteries. As our electron microscopy experiments showed, within the vessels VICs are closely associated with SMCs, which may suggest that they can communicate with nearby SMCs and play a role in the transmission of the electrical or chemical signals by means of contacts of processes with bodies of surrounding SMCs. Gastrointestinal ICCs can serve as intermediaries between nerves and SMCs [7]; also rabbit portal vein VICs were shown to release some vasoactive substance, which could depolarize nearby SMCs. That these have a place in the function of VICs in cerebral arteries, is yet to be established.

Our results strongly indicate that VICs are constitutively present in the wall of the RMCAs. These cells express several proteins considered to be markers of SMCs so likely VICs develop from the same precursor as SMCs. VICs represent a unique population of cells and we believe they may play an important role in blood vessels. At this stage, it is too early to suggest a potential role of VICs in disease or remodelling of blood vessels; for this, the possibility of migration and/or proliferation of VICs needs to be studied. We also believe that further comparative studies of genes and proteins expressed in both VICs and SMCs are also required as a next step to establish the role of VICs in blood vessels.

Acknowledgements

References

1. **Maiellaro K**, **Taylor WR**. The role of the adventitia in vascular inflammation. *Cardiovasc Res.* 2007; 75: 640–8.

2. **Owens GK**. Regulation of differentiation of vascular smooth muscle cells. *Physiol Rev.* 1995; 75: 487–517.

3. **Owens GK**, **Kumar MS**, **Wamhoff BR**. Molecular regulation of vascular smooth muscle cell differentiation in development and disease. *Physiol Rev.* 2004; 84: 767–801.

4. **Harhun MI**, **Gordienko DV**, **Povstyan OV**, *et al*. Function of interstitial cells of Cajal in the rabbit portal vein. *Circ Res.* 2004; 95: 619–26.

5. **Pucovsky V**, **Moss RF**, **Bolton TB**. Non-contractile cells with thin processes resembling interstitial cells of Cajal found in the wall of guinea-pig mesenteric arteries. *J Physiol.* 2003; 552: 119–33.

6. **Harhun MI**, **Pucovsky V**, **Povstyan OV**, *et al*. Interstitial cells in the vasculature. *J Cell Mol Med.* 2005; 9: 232–43.

7. **Sanders KM**. A case for interstitial cells of Cajal as pacemakers and mediators of neurotransmission in the gastrointestinal tract. *Gastroenterology.* 1996; 111: 492–515.

8. **Harhun M**, **Gordienko D**, **Kryshtal D**, *et al*. Role of intracellular stores in the regulation of rhythmical $[Ca^{2+}]_i$ changes in interstitial cells of Cajal from rabbit portal vein. *Cell Calcium.* 2006; 40: 287–98.

9. **Povstyan OV**, **Gordienko DV**, **Harhun MI**, *et al*. Identification of interstitial cells of Cajal in the rabbit portal vein. *Cell Calcium.* 2003; 33: 223–39.

10. **Pucovsky V**, **Harhun MI**, **Povstyan OV**, *et al*. Close relation of arterial ICC-like cells to the contractile phenotype of vascular smooth muscle cell. *J Cell Mol Med.* 2007; 11: 764–75.

11. **Sawaguchi A**, **Ide S**, **Goto Y**, *et al*. A simple contrast enhancement by potassium permanganate oxidation for Lowicryl K4M ultrathin sections prepared by high pressure freezing/ freeze substitution. *J Microsc.* 2001; 201: 77–83.

12. **Yoshida T**, **Owens GK**. Molecular determinants of vascular smooth muscle cell diversity. *Circ Res.* 2005; 96: 280–91.

13. **Epperson A**, **Hatton WJ**, **Callaghan B**, *et al*. Molecular markers expressed in cultured and freshly isolated interstitial cells of Cajal. *Am J Physiol Cell Physiol.* 2000; 279: C529–39.

14. **Wilkinson KD**, **Lee KM**, **Deshpande S**, *et al*. The neuron-specific protein PGP 9.5 is a ubiquitin carboxyl-terminal hydrolase. *Science.* 1989; 246: 670–3.

15. **Ferrara N**, **Gerber HP**, **LeCouter J**. The biology of VEGF and its receptors. *Nat Med.* 2003; 9: 669–76.

16. **Vanderwinden JM**, **Rumessen JJ**, **De Laet MH**, *et al*. CD34+ cells in human intestine are fibroblasts adjacent to, but distinct from, interstitial cells of Cajal. *Lab Invest.* 1999; 79: 59–65.

17. **Bosseloir A**, **Heinen E**, **Defrance T**, *et al*. Moabs MAS516 and 5B5, two fibroblast markers, recognize human follicular dendritic cells. *Immunol Lett.* 1994; 42: 49–54.

18. **Holness CL**, **Simmons DL**. Molecular cloning of CD68, a human macrophage marker related to lysosomal glycoproteins. *Blood.* 1993; 81: 1607–13.

19. **Hughes S**, **Chan-Ling T**. Characterization of smooth muscle cell and pericyte differentiation in the rat retina *in vivo*. *Invest Ophthalmol Vis Sci.* 2004; 45: 2795–806.

20. **Shmelkov SV**, **St Clair R**, **Lyden D**, *et al*. AC133/CD133/Prominin-1. *Int J Biochem Cell Biol.* 2005; 37: 715–9.

21. **Reynolds DS**, **Stevens RL**, **Gurley DS**, *et al*. Isolation and molecular cloning of mast cell carboxypeptidase A. A novel member of the carboxypeptidase gene family. *J Biol Chem.* 1989; 264: 20094–9.

22. **Bolton TB**, **Gordienko DV**, **Povstyan OV**, *et al*. Smooth muscle cells and interstitial cells of blood vessels. *Cell Calcium.* 2004; 35: 643–57.

23. **Costa ML**, **Escaleira R**, **Cataldo A**, *et al*. Desmin: molecular interactions and putative functions of the muscle intermediate filament protein. *Braz J Med Biol Res.* 2004; 37: 1819–30.

24. **Kilarski WW**, **Jura N**, **Gerwins P**. An *ex vivo* model for functional studies of myofibroblasts. *Lab Invest.* 2005; 85: 643–54.

25. **Geiger B**. Membrane-cytoskeleton interaction. *Biochim Biophys Acta.* 1983; 737: 305–41.

26. **Kumar MS**, **Owens GK**. Combinatorial control of smooth muscle-specific gene expression. *Arterioscler Thromb Vasc Biol.* 2003; 23: 737–47.

27. **Small JV**, **Gimona M**. The cytoskeleton of the vertebrate smooth muscle cell. *Acta Physiol Scand.* 1998; 164: 341–8.

28. **Bobryshev YV**. Subset of cells immunopositive for neurokinin-1 receptor identified as arterial interstitial cells of Cajal in human large arteries. *Cell Tissue Res.* 2005; 321: 45–55.

29. **Hinescu ME**, **Popescu LM**, **Gherghiceanu M**, *et al*. Interstitial Cajal-like cells in rat mesentery: an ultrastructural and immuno-histochemical approach. *J Cell Mol Med.* 2008; 12: 260–70.

30. **Worth NF**, **Rolfe BE**, **Song J**, *et al*. Vascular smooth muscle cell phenotypic modulation in culture is associated with reorganisation of contractile and cytoskeletal proteins. *Cell Motil Cytoskeleton.* 2001; 49: 130–45.

31. **Frid MG**, **Dempsey EC**, **Durmowicz AG**, *et al*. Smooth muscle cell heterogeneity in pulmonary and systemic vessels. Importance in vascular disease. *Arterioscler Thromb Vasc Biol.* 1997; 17: 1203–9.

32. **Jones BA**, **Aly HM**, **Forsyth EA**, *et al*. Phenotypic characterization of human smooth muscle cells derived from atherosclerotic tibial and peroneal arteries. *J Vasc Surg.* 1996; 24: 883–91.

33. **Hao H**, **Ropraz P**, **Verin V**, *et al*. Heterogeneity of smooth muscle cell populations cultured from pig coronary artery. *Arterioscler Thromb Vasc Biol.* 2002; 22: 1093–9.

34. **Fujii K**, **Heistad DD**, **Faraci FM**. Vasomotion of basilar arteries *in vivo*. *Am J Physiol* 1990; 258: H1829–34.

35. **Dirnagl U**, **Lindauer U**, **Villringer A**. Nitric oxide synthase blockade enhances vasomotion in the cerebral microcirculation of anesthetized rats. *Microvasc Res.* 1993; 45: 318–23.

36. **Haddock RE**, **Grayson TH**, **Brackenbury TD**, *et al*. Endothelial coordination of cerebral vasomotion *via* myoendothelial gap junctions containing connexins 37 and 40. *Am J Physiol Heart Circ Physiol.* 2006; 291: H2047–56.